Evidential grids with semantic lane information for intelligent vehicles

Chunlei Yu, Véronique Cherfaoui, Philippe Bonnifait

Evidential grids with semantic lane information for intelligent vehicles

Chunlei Yu[1], Véronique Cherfaoui[1], Philippe Bonnifait[1]

***Abstract*—Occupancy grids are popular in autonomous navigation for encoding obstacle information into grid cells to provide real-time environmental models. However, very few studies have been carried out on encoding lane and traffic information in grids. This information refines the world model up to the lane level which is important in many situations to enable vehicles to follow basic road rules, such as lane keeping or lane changes in case of overtaking for instance. Usual approaches consist in detecting lane boundaries using on-board cameras or lidars but the problem is tricky when the road is multi-lanes or in challenging weather conditions. In this work, we propose to tackle this problem by using a vectorial prior map that stores detailed lane level information. We take advantage of the pose estimation from a localization solver and propagate the estimation uncertainty over the grids cells. Both Bayesian and Evidential models are presented and some of their special characteristics are highlighted and compared. Real results carried on public roads with the same real-time software are reported to support the comparison.**

I. Introduction

In this paper, a grid-based approach is proposed to tackle the lane level perception for autonomous navigation. When running on a multi-lane road, the host vehicle needs semantic lane information to plan trajectories conforming to road rules, this is the reason why many lane detection methods have been studied and developed [1][2][3][4]. Nevertheless, lane detection methods relying on vision and lidar systems perform badly to extract parallel multi-lanes particularly in challenging weather conditions. In this work, we propose to take advantage of a prior maps to have access to lane level resources such as lane borders or lane orientations (in the sense of driving direction). With such detailed prior maps, a lane information can be easily retrieved once good localization (position and heading) with reliable confidence information is obtained. Advantages can be numerous: the map can provide accurate and integrated information for reliable navigation; the semantic lane information is easily accessible; no distance limit for map information, compared to even high definition sensors, since they all have a limited detection distance.

Occupancy grids [5][6][7][8] focus on the management of obstacle information into grid cells, in this work, we also propose to encode the lane information into spatial grids. One can interpret this lane information as a semantic meaning encoded in the cells. From the host vehicle's point of view, the navigable space is made up of the accessible lanes having a driving direction compatible with the vehicle orientation. Lanes with opposite direction and space outside of the road are non-navigable. So, let consider a frame of discernment defined as $\Omega = \{Ego, Accessible, Forbidden\}$. It contains minimal information allowing a vehicle to perform lane level navigation. In lane grids, every cell is filled with a belief state which characterizes the semantic lane information.

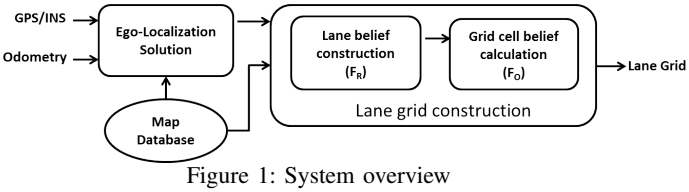

Figure 1: System overview

Fig 1 shows the whole process to construct Lane Grid. The Ego-localization system provides the pose information (position and heading) of the ego vehicle. The estimated pose has to be reliable, which implies that the true pose of the host vehicle has to be included in some estimated uncertainty bound. There exists two kinds of uncertainty in the process which come respectively from the estimated pose and from the map. In the current approach, we consider that the map is accurate and the one used in the experiments have been made with high-grade mobile mapping sensors. The pose uncertainty is therefore the predominant uncertainty which has to be taken into account.

The contributions of this work are a analysis of the propagation of pose uncertainties into the grid construction process, the developments of both probabilistic and evidential approaches to encode semantic lane information from maps, and a demonstration and comparison of the two approaches with real road data.

The paper is organized as follows: Section II gives a detailed illustration of uncertainty analysis concerning the two steps to construct lane grids. The two steps are detailed in sections III and IV. In section V, experimental results are shown and compared. Finally, conclusions are given in section VI.

II. Uncertainty analysis

The term $Belief$ used in Fig 1 can have different meanings depending on the considered approach. In the probabilistic approach, $Belief$ refers to $Probability$, in the evidential one, $Belief$ means $Mass$, since $Mass$ is the basic belief assignment in the Dempster-Shafer's theory.

A. Coordinates definition for different uncertainties

Let denote F_O the global frame, it has an origin O close to the navigation area to work in 2D. A road-oriented frame

[1] The authors are with *Sorbonne Universités, Université de Technologie de Compiègne*, *CNRS Heudiasyc UMR* 7253*, France*

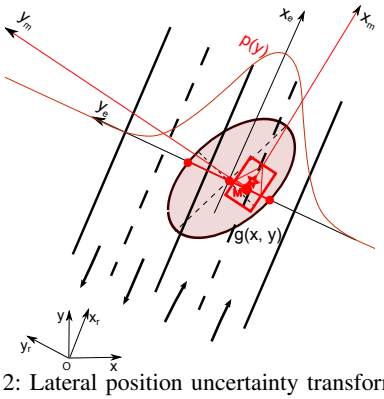

Figure 2: Lateral position uncertainty transformation

F_R [9] has the same origin as the global frame but with its x-axis pointing in the direction of the road. It is actually a rotated version of the global frame. The body frame of the vehicle F_M is defined at the center of the vehicle's rear axle with an origin denoted M. Note that M has not a deterministic location in F_O or F_R because of the estimation uncertainty, but the uncertainty has to be well quantified. In Fig 2, a position M with an uncertainty ellipse $g(x,\, y)$ is given for illustrating purpose.

B. Uncertainty of vehicle position in the road frame

The lane belief distribution characterizes the states of the lanes based on the estimated pose of the host vehicle on the road. This process is carried out in the road-oriented frame F_R. To characterize the lane states, one has to decide first on which lane the host vehicle is located. This requires the knowledge of the lateral position with respect to the road. The pose is estimated in the global frame with a 2D ellipse uncertainty $g(x,\, y)$ as shown in Fig 2. In the frame (x_e, y_e) defined at the estimated position, the lateral position uncertainty to construct the lane belief distribution is perpendicular to the lane direction, i.e, along the axis y_e. The lateral uncertainty is represented by $p(y)$ in Fig 2.

To calculate this uncertainty, suppose that the position uncertainty is represented in F_O by the following covariance matrix:

$$^{O}\mathbf{P} = \begin{bmatrix} {}^{O}p_{11} & {}^{O}p_{12} \\ {}^{O}p_{12} & {}^{O}p_{22} \end{bmatrix}$$

The transformation of this uncertainty into the road-oriented frame F_R is given by:The lateral uncertainty is represented by $p(y)$ in Fig 2.

$$^{\mathbf{R}}\mathbf{P} = \begin{bmatrix} {}^{R}p_{11} & {}^{R}p_{12} \\ {}^{R}p_{12} & {}^{R}p_{22} \end{bmatrix} = \mathbf{R} \cdot {}^{O}\mathbf{P} \cdot \mathbf{R}^{T} \qquad (1)$$

where $\mathbf{R} = \begin{bmatrix} cos(\psi) & sin(\psi) \\ -sin(\psi) & cos(\psi) \end{bmatrix}$ is the rotation matrix in which ψ is the heading of the road.

C. Uncertainty of grid cells in global frame

Fig 3 illustrates the uncertainty in the computation of the belief distribution for the grid cells. $b_1 \sim b_6$ represent the belief distribution for each lane (the case where the position

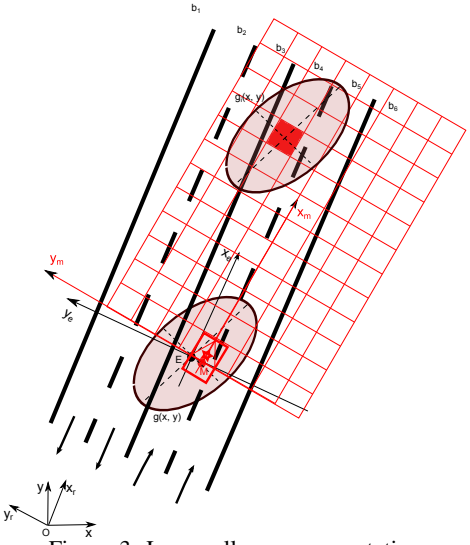

Figure 3: Lane cell mass computation

distribution extends to outside of the road is taken into consideration, each side of the space outside the road is taken as a lane). To illustrate the model, let us imagine that the true position of vehicle is M and the lane grid is shown in red.

Let us compute the uncertainty denoted $g_i(x,\, y)$ of the red cell i displayed in Fig 3. The coordinates vector of cell i in F_M is ${}^{M}X_i = \begin{bmatrix} {}^{M}x_i & {}^{M}y_i \end{bmatrix}^{T}$. Transformed into F_O:

$$^{O}X_i = \begin{bmatrix} {}^{O}x_i \\ {}^{O}y_i \end{bmatrix} = {}^{\mathrm{O}}\mathbf{R}_{\mathrm{M}} \cdot \begin{bmatrix} {}^{M}x_i \\ {}^{M}y_i \end{bmatrix} + \begin{bmatrix} {}^{O}x_M \\ {}^{O}y_M \end{bmatrix} = h(\theta) \qquad (2)$$

where ${}^{\mathrm{O}}\mathbf{R}_{\mathrm{M}}$ is the rotation matrix from F_M to F_O, ${}^{\mathrm{O}}\mathbf{R}_{\mathrm{M}} = \begin{bmatrix} \cos(\theta) & -\sin(\theta) \\ \sin(\theta) & \cos(\theta) \end{bmatrix}$, $\begin{bmatrix} {}^{O}x_M \\ {}^{O}y_M \end{bmatrix}$ is the position of M in F_O. θ is the estimated heading angle of the vehicle. $({}^{M}x_i,\, {}^{M}y_i)$ has no uncertainty because the positions of the cells are known. Thus, the position uncertainty of the cell in the global frame comes only from the pose of the vehicle $({}^{O}x_M,\, {}^{O}y_M,\, \theta)$.

To understand the effect of the uncertainty transformation, let us suppose that the heading angle θ is decorrelated from the position $({}^{O}x_M,\, {}^{O}y_M)$. This allows analyzing the influence separately. Firstly, the uncertainty from $({}^{O}x_M,\, {}^{O}y_M)$ is propagated uniformly since the relation is linear, if we suppose the heading angle has no uncertainty.

Now, suppose the heading angle has some uncertainty and the position is perfectly known. The covariance matrix of ${}^{O}\mathbf{X}_i$ can be computed in close form as:

$$\begin{aligned} Var({}^{O}\mathbf{X}_i | Var(\begin{bmatrix} {}^{O}x_M \\ {}^{O}y_M \end{bmatrix}) = 0) &= \left[\frac{dh}{d\theta}\right] \cdot var(\theta) \cdot \left[\frac{dh}{d\theta}\right]^{T} \\ &= var(\theta) \cdot \begin{bmatrix} u(\theta) & t(\theta) \\ t(\theta) & v(\theta) \end{bmatrix} \end{aligned} \qquad (3)$$

where

$$u(\theta) = (-\sin(\theta) \cdot {}^{M}x_i - \cos(\theta) \cdot {}^{M}y_i)^2$$

$$v(\theta) = (\cos(\theta) \cdot {}^{M}x_i - \sin(\theta) \cdot {}^{M}y_i)^2$$

$$t(\theta) = \sin\theta \cdot \cos\theta \cdot (({}^{M}y_i)^2 - ({}^{M}x_i)^2) + {}^{M}x_i \cdot {}^{M}y_i \cdot ((\sin\theta)^2 - (\cos\theta)^2)$$

One can remark that the uncertainty of the heading angle θ is not uniformly propagated to grid cells. The uncertainty is a

function of $({}^{M}x_i, {}^{M}y_i)$ which means that the position of the cell in F_M determines the shape of the uncertainty in F_O. The farther a cell is located, the larger the uncertainty is in the x direction. The uncertainty in the y direction (with the same y coordinate) increases when x coordinate augments. Thus, in general, we can conclude that the uncertainty of one cell due to heading error increases in the x direction.

For the general case, let denote $Var({}^{O}\mathbf{X}_i)$ the uncertainty of cell i in the global frame. $f({}^{O}x_M, {}^{O}y_M, \theta)$ denotes the transformation (Eq 2). At the first order, we have:

$$g_i(x, y) = Var({}^{O}\mathbf{X}_i) = \left[\frac{\delta f}{\delta {}^{O}\mathbf{X}_i}\right] \cdot {}^{O}\mathbf{P_{33}} \cdot \left[\frac{\delta f}{\delta {}^{O}\mathbf{X}_i}\right]^T, \quad (4)$$

where ${}^{O}\mathbf{P_{33}}$ represents the covariance matrix of the 2D pose $({}^{O}x_M, {}^{O}y_M, \theta)$ and $\left[\frac{\delta f}{\delta {}^{O}\mathbf{X}_i}\right]$ the Jacobian.

III. Lane Belief Construction

The lane belief distribution characterizes the lane status from the estimated pose of the vehicle. It is based on the road rules stored in the map. A multi-hypothesis probabilistic approach is proposed. So, a lane belief serves both for the probabilistic and evidential approaches in the grid cell belief calculation process. In general, the belief level is denoted as $B()$ in this part, which can be transformed to $P()$ and $m()$ in the probabilistic and evidential approaches respectively. Let $B(i, A)$ be the belief of state A for lane i.

A. Multi-hypothesis approach

Due to the lateral uncertainty, one can make an error when deciding on which lane the host vehicle is located. To tackle this problem, we consider from this uncertainty every possibility concerning which lane is Ego. The algorithms considering all the hypotheses of belief distribution are given in Algo 1, 2 and 3 shown in the Appendix. In summary, the method considers every lane where the host vehicle can be located, then computes for each case the belief supporting that particular hypothesis.

The approach is illustrated in Fig 2. $p(y)$ represents the lateral position distribution in F_R. The position has a large lateral uncertainty and the Gaussian distribution covers multi-lanes. Fig 4 gives an illustrative example on a four-lane road with solid lane marking in the middle (A means $Accessible$, E means Ego, F means $Forbidden$). In Fig 4a, lane 3 is assumed to be Ego and then the belief is calculated as the integral of the pose distribution over the lane. Thus, $B(3, Ego) = P(Lane\{3\} = Ego) = \int_K^P p(y)dy$. This belief is propagated to the other lanes based on the hypothesis that the map is accurate and with no attribute error. Once lane 3 is regarded as Ego, lane 4 should be $Accessible$ with the same amount of belief based on the relationship of the two lanes on the map, $B(4, Accessible) = P(Lane\{3\} = Ego)$. The same rule applies to lane 1 and lane 2. These two lanes can only be $Forbidden$, thus $B(1, Forbidden) = B(2, Forbidden) = P(Lane\{3\} = Ego)$.

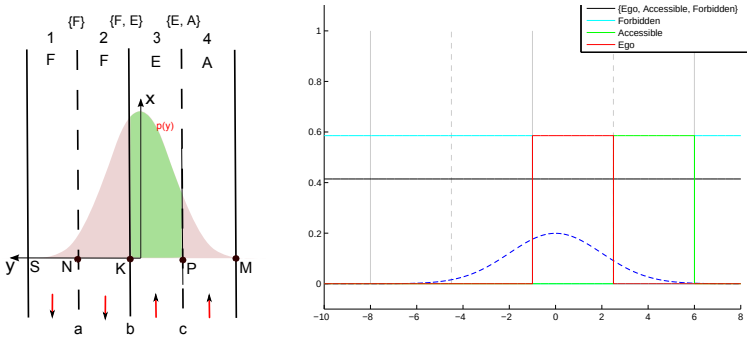

(a) Example one (b) Belief distribution

Figure 4: Multi-hypothesis algorithm illustration

To illustrate the model, a simulation has been done given the same road situation. The result of the example is shown in Fig 4b.

B. Belief accumulation

Every hypothesis is tackled independently, and each hypothesis brings new belief on different propositions. If different hypotheses would have contributed to the same proposition, the belief would be accumulated. The final belief distribution is shown in Fig 5. The belief accumulation is mostly highlighted from the $Forbidden$ mass outside the road. The lateral pose distribution is limited to the road area, thus $Forbidden$ belief accumulates to 100% outside the road, which is conform with reality.

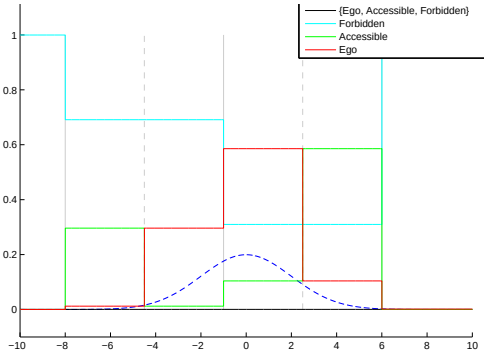

Figure 5: Final lane belief distribution in the cross-track direction

IV. Grid Cell Belief Calculation

In this section, the formalism to calculate the belief state is detailed, for both probabilistic and evidential approaches.

A. Probabilistic approach

In this framework, probabilities can only be assigned to singletons in Ω. With the lane probability distribution already composed, we need to model where locates the cell to compute its probability distribution. To take advantage of the lane belief distribution constructed in section III, the probability

of lane i to be in the state A is $P(S_{l_k} = A) = B(k, A)$. We define two properties for each cell in the grid: L_i and S_i. They indicate respectively the lane index and the state of cell i. Thus $L_i \in (1, 2, \ldots n)$ where n represents the number of lanes, and $S_i \in \Omega$.

The probability of the red cell i in Fig 3 being located in lane k can be calculated as:

$$P(L_i = k) = \iint_{(x,y \in Lane_k)} g_i(x, y) dx dy. \tag{5}$$

According to the total probability law, the probability of the state A for the cell is computed as:

$$P(S_i = A) = \sum_{k=1}^{n} P(S_i = A \,|\, L_i = k) \cdot P(L_i = k),\ A \in \Omega.$$

With the part $P(L_i = k)$ already tackled in Eq. 5, the problem resides in computing the part $P(S_i = A \,|\, L_i = k)$. Suppose the state for lane k is denoted as S_{l_k}, the first part can be developed into:

$$P(S_i = A \,|\, L_i = k) = P(S_i = A \,|\, S_i = S_{l_k})$$

because if one cell lies in lane k, then it has the same state as the lane k. Moreover,

$$P(S_i = A \,|\, S_i = S_{l_k}) = P(S_{l_k} = A) = B(k, A).$$

B. Evidential approach

Dempster-shafer's theory provides a generalized way to deal with uncertainty. The singletons in Ω are mutually exclusive. The power set is defined as:

$$2^{\Omega} = \{\emptyset, Ego, Accessible, Forbidden, \{Ego, Accessible\}, \{Ego, Forbidden\}, \{Accessible, Forbidden\}, \Omega\}.$$

One advantage of the evidential representation is that one can attribute mass to any subset of the frame of discernment. For example $\{Ego, Accessible\}$ is not null in the case when the mass supports both Ego and $Accessible$, but there is not enough information to tell whether the mass should be assigned to Ego or $Accessible$.

If one cell lies inside one lane, then it should have the same mass distribution as the lane:

$$m^i = m_k,\ \text{if}\, C_i \in Lane_k$$

in which m^i and m_k represent respectively the mass distribution of cell i and $Lane_k$. One should note that the belief distribution constructed in section III can be adopted here as $m_k(A) = B(k, A)$.

Due to the position uncertainty $g_i(x, y)$, the cell i can be located within each lane with a certain confidence level which can be computed by:

$$\alpha_k^i = \iint_{(x,y \in Lane_k)} g_i(x, y) dx dy. \tag{6}$$

This confidence level is applied to discount the mass distribution of each lane m_k [10].

The mass distribution for the cell i belonging to lane k is m_k^i and is computed:

$$\begin{aligned} m_k^i(A) &= \alpha_k^i \cdot m_k(A), \quad A \subseteq \Omega,\ A \neq \Omega \\ m_k^i(\Omega) &= \alpha_k^i \cdot m_k(\Omega) + 1 - \alpha_k^i \end{aligned}$$

Fusing all the information provided by all the lanes, we can now compute the mass distribution for cell i by:

$$m^i = \circledcirc_k m_k^i,\ k = 1, 2, \ldots, n \tag{7}$$

in which k is the lane index, n is the number of lanes.

The fusion operator $\circledcirc$ proposed in [11] is defined as:

$$\begin{cases} (m_1 \circledcirc m_2)(A) = \sum_{B \cap C = A \neq \emptyset} m_1(B) \cdot m_2(C) \\ (m_1 \circledcirc m_2)(A) = \sum_{B \cap C = \emptyset,\, B \cup C = A} m_1(B) \cdot m_2(C) \end{cases} \quad A,\, B,\, C \subset \Omega$$

The specialty of this operator is that the conflicting mass is put into union states. In our case, this conflicting mass is due to the position uncertainty. If, in the fusion process, conflicting information is generated, we assume that the evidence supports the mass distribution of the two fused hypotheses. This highlights an advantage of the evidential approach which will be demonstrated in the results.

V. Real road experiments and results

Real road experiments have been done with an equipped vehicle of the Lab shown in Fig 6. A pre-constructed map with a negligible error level has been used. In the map, any road is explicitly described with lane information, including lane markings and road boundaries. The lane markings are distinguished in the map with different attributes. This feature is important to determine the lane state. A GPS system with RTK corrections provided accurate positioning information with high confidence during the tests.

Figure 6: Experimental vehicle used in this work

To qualitatively evaluate the result, the approach proposed in [12] is adopted. The retro-projection of the Lane Grid on the scene image helps support a qualitative evaluation. The essential purpose of this method is to analyze and evaluate the correspondence between the Lane Grid and the scene observed by the camera.

The grids are of $40 * 16$ meters in length and width and the cells size is $(0.1 * 0.1)$ meters. For denotation purpose, we herein use $(\sigma_x,\, \sigma_y\,, \sigma_\theta)$ as the 2D pose uncertainty. The whole approach has been implemented in C++. A video illustrating the results of a whole test on public roads with lane changes is accessible on line[1]. The results are shown in the form of a RGB image. The advantage is that the belief level is reflected by the RGB color brightness. A brighter color means a higher believe level. In the following, we focus on one particular sample and we compare the two approaches.

A. Probabilistic lane grid result

[1]https://www.youtube.com/watch?v=0Cl4m2cua_c&feature=youtu.be

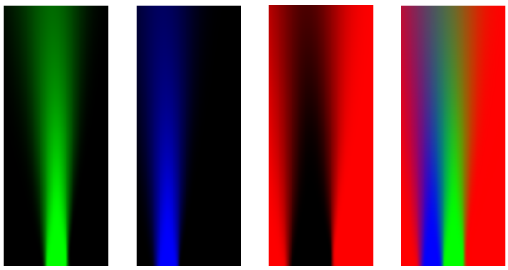

(a) Ego (b) Accessible (c) Forbidden (d) All

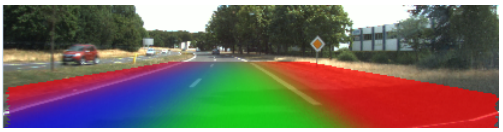

(e) Retro-projection on the front-looking image

Figure 7: Probabilistic approach

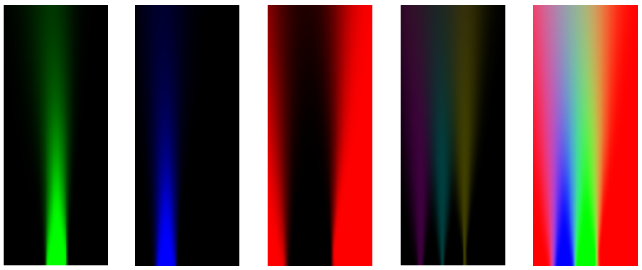

(a) Ego (b) Accessible (c) Forbidden (d) Union (e) Singleton

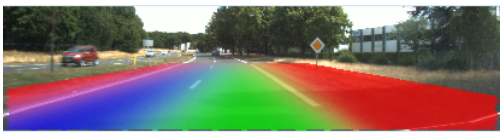

(f) Retro-projection of all singleton masses on the image

(g) Retro-projection of the union of masses on the image

Figure 8: Evidential approach

Fig 7 shows the resulting probabilistic grids with the following pose uncertainty ($\sigma_x = 0.3m$, $\sigma_y = 0.2m$, $\sigma_\theta = 0.1radians$). The Ego, $Accessible$, and $Forbidden$ probabilities along each lane become smaller as the distance of the cells to the host vehicle gets larger. However, the space covered by the probability distribution extends to outside of each lane, which means that the probability becomes more dispersed. The uncertainty propagation explained in section II is the reason for this phenomenon. It is clear that if one cell has a larger position uncertainty, it ought to have more ambiguous probability distribution. As the approach takes into account the 2D pose uncertainty, the cells at farther distance tend to have larger uncertainty. The combined probability shown in Fig 7d further reflects this phenomenon. One can remark clearly that cells close to the host vehicle tend to have just single state probability, whereas at farther distance, the probability distribution can become very ambiguous.

The retro-projection of the lane grid on the image in Fig 7e gives a qualitative result evaluation. One can see the result is valid given the correspondence of the lane grid projected on the image.

B. Evidential lane grid result

Fig 8 displays the results of the evidential approach with the same pose uncertainty. The belief of the states of the lanes gradually decreases as the distance of the cells to the host vehicle becomes larger. From the mass in the union states shown in Fig 8d, one can remark that some quantity of mass is put in the union states, which is displayed by the combination of colors. In Fig 8d, yellow, cyan and magenta colors represent respectively the mass in $\{Ego, Forbidden\}$, $\{Ego, Accessible\}$ and $\{Accessible, Forbidden\}$. The fact that farther cells have larger uncertainty is more clearly reflected in this image, as the union mass area becomes wider in the farther space. In Fig 8g the retro-projection of union mass is demonstrated, this result directly shows the fact that the union mass is mainly focused on the cells that are close to the lane markings.

C. Influences of position and angle uncertainties

Based on the discussion in section II, the position uncertainty is propagated uniformly over the lane grid, whereas the angle uncertainty is not. In this section, we show the results which reflect these two propagations of uncertainties. The uncertainty propagation effects have same impact on the Bayesian and Evidential approaches, herein we choose the evidential approach for illustration since more visual results can be demonstrated. In Fig 9 the results with only position uncertainties are displayed. The uncertainties are respectively $(0.3m, 0.2m, 0.0radians)$ and $(1.0m, 1.0m, 0.0radians)$ in Fig 9a and Fig 9b. Based on these results, one can remark that with position uncertainty, the fading effect of each lane states over each lane is uniform all along the lane space, even the distance get larger. With larger position uncertainty, the mass level for lane states get lower, which means less confident about the lane states for the grid cells.

The Fig 10 shows two cases of different angle uncertainties when there is no position uncertainty. The uncertainties are respectively $(0.0m, 0.0m, 0.05radians)$ and $(0.0m, 0.0m, 0.1radians)$ in Fig 10a and Fig 10b. The effect of larger angle uncertainty is reflected by the lower mass level over the space in larger distance in Fig 10b. With larger angle uncertainty, the cells in Fig 10b have larger uncertainties, thus their mass dispersion is more significant, which results in the more ambiguous lane grid.

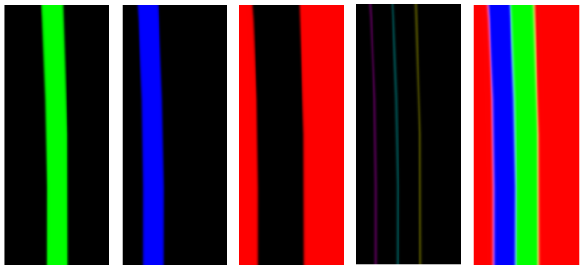

(a) small position uncertainty

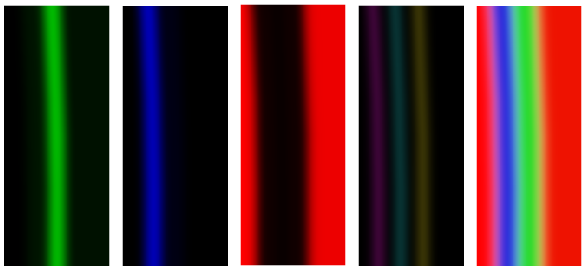

(b) large position uncertainty

Figure 9: Results with only position uncertainties

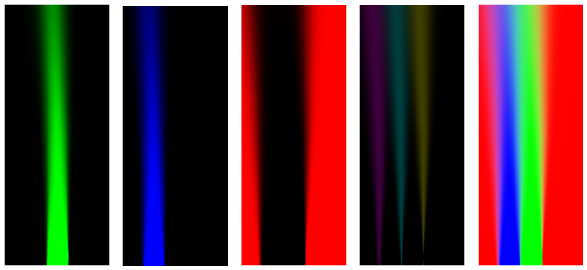

(a) small angle uncertainty

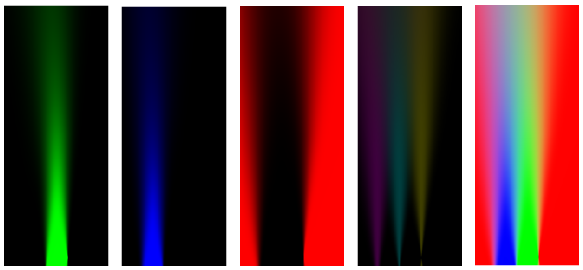

(b) large angle uncertainty

Figure 10: Results with only angle uncertainties

D. Comparison between the two approaches

The evidential approach provides richer information than the probabilistic one. Indeed, it puts beliefs into union states if the belief in each single state is not clear. Ignorance is explicitly quantified by the $Unknown$ mass. Moreover, the evidential approach provides a flexible method to tackle conflicting information which also brings useful information. Here, the conflicting mass corresponds to the lane markings.

Another essential difference resides in the decision process. In a probabilistic approach, decision is classically made by selecting the maximum probability. Thus, the decision is always among these three states, no matter how uncertain

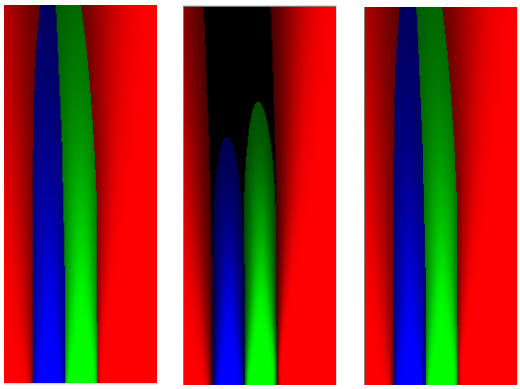

(a) Proba (b) Evidence (c) Pignistic

Figure 11: Decision grids (used by client applications)

the information is. However, in the evidential approach, it is authorized to explicitly announce ignorance when there is too large uncertainty. Fig 11 shows the decision grids of the results shown in Fig 7 and in Fig 8. In these decision grids, the belief level is kept to reflect the uncertainty level. Fig 11a shows the max of probabilities. The Ego and $Accessible$ lanes at farther distance become more narrow. This phenomenon is due to the fact that the probability dispersion in this area becomes larger and the $Forbidden$ belief outside the road has larger influence which leads to $Forbidden$ belief invasion into lane space. Fig 11b shows a decision grid based on the maximum of mass of evidence. One can remark that over the far away space, the cells are $Unknown$, which means that no decision can be made in this area due to the lack of information. This is a great advantage for a path planning process, since, as this evidential decision grid provides explicitly ignorant information, no risky trajectory can be planned.

In Fig 11c shows another decision grid based on pignistic probability [13], commonly used to transform evidence masses in probabilities. One can remark that this grid looks almost exactly the same as the probabilistic decision grid in Fig 11a. In fact, the ratio of identical decision of these two grids reaches 99.992%. This result validates the way uncertainty is handled in the proposed evidential grid mechanism as it conducts to the same probabilistic conclusions.

VI. Conclusion

A new approach to characterize lane information and semantic road rules into grid cells has been proposed. A prior lane-level map is used to extract lane information based on the pose provided by a localization system. As any localization system provides uncertain information, the uncertainty propagation over the grid has been analyzed and methods to build probabilistic and evidential lane grids have been proposed. Real road results have been reported and compared with a qualitative evaluation based on the retro-projection of the 2D grids on ground truth images. The evidential framework relying on mass discounting has

been validated trough decision grids comparisons. It has the advantage of explicitly managing ignorance which is clearly an added value for safe autonomous navigation.

REFERENCES

[1] M. Thuy and F. P. Leon, "Lane detection and tracking based on lidar data," *METROLOGY AND MEASUREMENT SYSTEMS*, vol. 11, 2010.

[2] M. Aly, "Real time detection of lane markers in urban streets," *Intelligent Vehicles Symposium, IEEE*, vol. 6, pp. 7 – 12, 2008.

[3] A. Parajuli, M. Celenk, and H. B. Riley, "Robust lane detection in shadows and low illumination conditions using local gradient freatures," *Open Journal of Applied Sciencecs*, vol. 7, pp. 68 – 74, 2013.

[4] G. Cui, J. Wang, and J. Li, "Robust multilane detection and tracking in urban scenarios based on lidar and mono-vision," *IET Image Processing*, vol. 11, 2013.

[5] A. Elfes, "Using occupancy grids for mobile robot perception and navigation," *Computer*, vol. 22, no. 6, pp. 46 – 57, 1989.

[6] D. Pagac, E. M.Nebot, and H. Durrant-Whyte, "An evidential approach to map-building for autonomous vehicles," *IEEE Transactions on Robotics*, vol. 7, pp. 623–629, 1998.

[7] C. Coue, C. Pradalier, C. Laugier, T. Fraichard, and P. Bessiere, "Bayesian occupancy filteing for multitarget tracking : an automotive application," *International Journal of robotics research*, vol. 25, no. 1, pp. 19–30, 2006.

[8] J. Moras, V. Cherfaoui, and P. Bonnifait, "Credibilist occupancy grids for vehicle perception in dynamic environments," *IEEE International Conference on Robotics and Automation*, vol. 6, 2011.

[9] P. B. Zui Tao, "Road invariant extended kalman filter for an enhanced estimation of gps errors using lane markings," *IEEE/RSJ International Conference on Intelligent Robots and Systems*, vol. 6, 2015.

[10] M. Kurdej and V. Cherfaoui, "Conservative, proportional and optimistic contextual discounting in the belief functions theory," *16th International Conference on Information Fusion*, vol. 7, pp. 2012–2018, 2013,.

[11] D. Dubois and H. Prade, "Representation and combination of uncertainty with belief functions and possibility measures," *Computer intelligence*, vol. 4, pp. 244–264, 1988.

[12] J. Moras, S. A. R. F., V. Drevelle, G. Dherbomez, V. Cherfaoui, and P. Bonnifait, "Drivable space characterization using automotive lidar and georeferenced map information," *Intelligent Vehicles Symposium*, vol. 6, 2012.

[13] P. Smets, "Decision making in the tbm: the necessity of the pignistic transformation," *Int. Journal of Approximate Reasoning*, vol. 38, pp. 133–147, 2005.

APPENDIX

Algorithm 1 Multi-hypothesis Lane Belief Distribution Construction

input: Map, grid size($gSize$), Pose(P), Pose uncertainty(COV)
output: Lane Belief Distribution

1. Check out the lane information from Map based on P and $gSize$
   N_l=lane number, N_m=marking number
   $marking\_continuity$ as (N_m * 1) vector. %indication of road rule
2. COV_r = Convert2Road(COV) %covariance in the road frame
   $p(y)$ = Norm(0, $COV_r(2,2)$) %Gaussian distribution
3. Compute each lane's span on the distribution, $span(i)$, i=(1, N_l)
4. Initialize $lane\_state$ as N_l * 1 vector
5. For each lane $lane_i$ in N_l
   initialize $lane\_state$ all as $Forbidden$
   $lane\_state$ = ComputeLaneState($lane\_state$, $lane_i$, $marking\_continuity$)
   For each lane $lane_j$ in N_l
   B($lane_j$, $lane\_state\_buffer(lane_j)$) += $\int_{span_i} p(y)$
   Endfor
   Endfor

Algorithm 2 Function Convert2Road

input: Pose uncertainty(COV), road cap ψ
output: COV_r %covariance in road frame

1. $Rotation = [\cos\psi \quad \sin\psi; -\sin\psi \quad \cos\psi]$
2. $COV_r = Rotation * COV * Rotation^T$

Algorithm 3 Function ComputeLaneState

input: $lane\_state$, $laneId$, $marking\_continuity$
output: $lane\_state$

1. $lane\_state(laneId)$ = Ego %when current lane is Ego
2. For each lane $lane_i$ in N_l
   IF $lane_i == laneId$
   continue
   Endif
   $state\_temp$ = Accessible
   IF $lane_i > laneId$
   For $markingId$ in $[laneId, lane_i - 1]$
   IF $marking\_continuity(markingId)$ == solid
   $state\_temp$ = Forbidden
   Endif
   Endfor
   Endif
   IF $lane_i < laneId$
   For $markingId$ in $[laneId - 1, lane_i]$
   IF $marking\_continuity(markingId)$ == solid
   $state\_temp$ = Forbidden
   Endif
   Endfor
   Endif
   $lane\_state(lane_i)$=$state\_temp$
   Endfor